

Microstep Stepper Motor Control Based on FPGA Hardware Implementation

Sorawat Chivapreecha and Kobchai Dejhan

Faculty of Engineering and Research Center for Communication and Information Technology
King Mongkut's Institute of Technology Ladkrabang, Bangkok 10520, Thailand
Tel: +66-2-326-4238, +66-2-326-4242, Fax. +66-2-326-4554; E-mail : {sorawat, kobchai}@telecom.kmitl.ac.th

Abstract: This paper proposes a design of stepper motor control in microstep driven mode using FPGA (Field Programmable Gate Array) for hardware implementation. The methods to drive stepper motor in microstep excitation mode are to control of the controlling currents in each phase windings of stepper motor with reference signals. These reference signals are used for controlling the current levels, the required variation of current levels with rotor position can be obtained from the ideal linear or sinusoidal approximations to the static torque-displacement ($T-\theta$) characteristic curve. In addition, the hardware implementation of stepper motor controller can be designed uses VHDL (Very high speed integrated circuits Hardware Description Language) and synthesis using an Altera FPGA, FLEX10K family, EPF10K20RC240-4 device as target technology and use MAX+PlusII program for overall development. A multi-stack variable-reluctance stepper motor of Sanyo Denki is used in the experiments.

Keywords: Microstep, Stepper Motor, Current Control, FPGA

1. INTRODUCTION

In high precision stepper motor applications, it is necessary to use motors with small steps whose size is imposed by the required resolution such as applications to printer, plotter, robot arm and etc. Furthermore, the operation of stepper motor in the full step size also causes to overshoot problem of the rotor position.

For the conventional full step drive, the equilibrium positions are defined by the alignment of stator and rotor teeth and are independent of current level. However, the microstep positions are critically dependent on the currents in each of the phase windings. The full step length of a stepper motor can be divided into smaller increments of rotor motion known as ministep or microstep by partially exciting several phase windings. If two phase currents are unequal, the rotor position will be shifted towards the stronger pole. This effect is utilized in the microstep excitation mode which subdivides the basic motor step by proportioning the current in two windings [1-2].

In this case, the step size is reduced and the lower-speed smoothness is dramatically improved. High resolution microstep drives divide the full motor step into 500 microsteps, giving 100,000 steps per revolution (a typical reduction is twenty microsteps per full step depend on type of motor). In this situation, the current pattern in the windings closely resembles two sine waves with 90 degrees phase shift between them.

2. MICROSTEP CURRENT REFERENCES USING $T-\theta$ CHARACTERISTICS

In regular step of stepper motor is arranged by energizing a certain number of motor windings (1 or 2 phases) and the rotor finds a minimum reluctance path that called a detent position. The level of current in each phase winding is usually fixed at the rated value of motor and motor step angle is fixed by the mechanical design of numbers of stator and rotor teeth.

In order to excite in microstep driven mode, sub-detent positions must be established between regular detent position. The currents in two or more phase windings have to be simultaneously controlled at discrete levels. Therefore, the main task of designing a micristep controller is to design of current controllers for each motor phase windings.

The reference signals used for control the current levels in each of phase windings can be obtained from the linear or sinusoidal approximations to the static torque-displacement ($T-\theta$) characteristic curve [3-4]. The restoring torque to maintain static equilibrium of stepper motor around a detent position is related to motor current (i) and displacement (θ) is given by

$$T = f(i, \theta) \quad (1)$$

and can be shown in Fig. 1

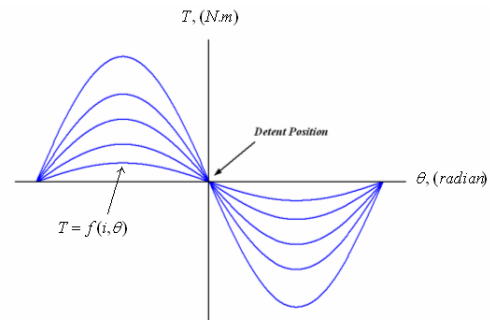


Fig. 1 Torque-displacement ($T-\theta$) characteristic curve

For the regular detent positions while torque is zero, are occurred at angle $n\theta_s$ where n is 1, 2, 3, ... and θ_s is regular step size. If sub-detent positions are required at angle $\theta = n\theta_s/m$ where m is number of microstep, current references for each phase windings have to be calculated from (1) and can be represented this function by linear or sinusoidal approximation to $T-\theta$ curve in Fig. 1 as shown in Fig. 2

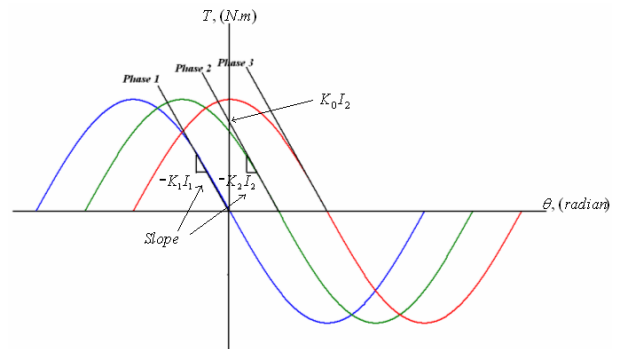


Fig. 2 Linear and sinusoidal approximation to $T-\theta$ curve

In order to approximate $T-\theta$ curves to be linear equations. Consider for phase winding 1 and 2, respectively and assume to linear magnetic circuit [1-3]. Each of phase torque can be expressed as

$$T_1 = -K_1 I_1 \theta \quad (2)$$

$$T_2 = -K_2 I_2 \theta + K_0 I_2 \quad (3)$$

Where I_1 and I_2 are currents, K_1 and K_2 are constant torque for phase winding 1 and 2, respectively. To establish sub-detent position for a microstep is desired at any angle θ , The summation of each phase torques must be zero, so that

$$T_1 + T_2 = 0 \quad (4)$$

Also, from (2)-(4) can be got

$$\theta = \frac{K_0 I_2}{K_1 I_1 + K_2 I_2} \quad (5)$$

Assume that original $T-\theta$ curve of each phase are identical, so that $K_1=K_2=K$. Also, the slope of $T-\theta$ curve at sub-detent is

$$\frac{d(T_1 + T_2)}{d\theta} = -K_1 I_1 - K_2 I_2 = -K(I_1 + I_2) \quad (6)$$

The slope of $T-\theta$ curve at new sub-detent must be same as original. Also, from (6) will be given as

$$I_1 + I_2 = 1 \quad (7)$$

Also, from (5), θ will be

$$\theta = \frac{K_0}{K} I_2 \quad (8)$$

Consequently, can be summarized as

$$I_1 = 1 - \frac{\theta}{\theta_s} \quad (9)$$

From (9), the current in phase 1 should be reduced at discrete steps and in phase 2 should be increased in equal steps to obtain microstep detent positions as shown in Fig. 3.

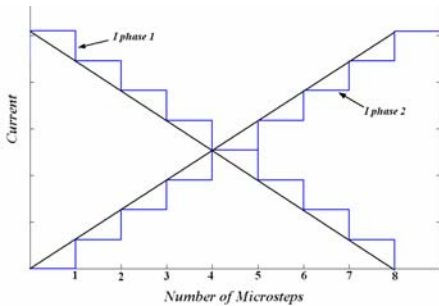


Fig. 3 Microstep currents waveform for $m=8$ in case of linear approximation

In order to approximate $T-\theta$ curves to sinusoidal, considering from Fig. 2 again. The phase torque 1 and 2 can be approximated [1-3] as follows,

$$T_1 = -T_0 I_1 \sin \theta \quad (10)$$

$$T_2 = T_0 I_2 \sin(\theta + \theta_s) \quad (11)$$

where T_0 is peak static torque and give $T_1+T_2=0$ at microstep detent position which will give

$$\frac{I_2}{I_1} = \frac{\tan \theta}{\tan \theta \cos \theta_s + \sin \theta_s} \quad (12)$$

To preserve the characteristic of $T-\theta$ curves for microstep mode, the restoring torque at any microstep detent must be equal to T_1 or T_2 . Also,

$$T_0 I_2 \sin(\theta' + \theta_s) - T_0 I_1 \sin \theta' = T_0 \sin\left(\frac{\theta_s}{m}\right) \quad (13)$$

where $\theta' = \theta - \frac{\theta_s}{m}$

Combine (12) and (13) and can be shown as

$$I_1 = \frac{\sin\left(\frac{\theta_s}{m}\right)}{\frac{\tan \theta}{\tan \theta \cos \theta_s + \sin \theta_s} \sin(\theta' + \theta_s) - \sin \theta'} \quad (14)$$

From (12) and (14) can be found that the current waveform pattern of I_1 and I_2 to obtain microstep detent positions as shown in Fig. 4 for microstep was subdivided by 16.

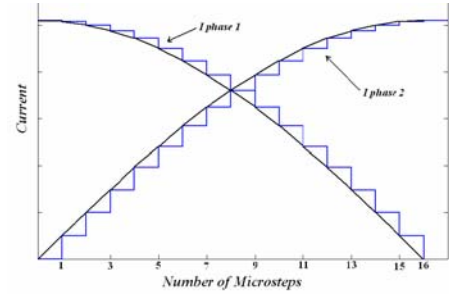


Fig. 4 Microstep currents waveform for $m=16$ in case of sinusoidal approximation

3. ARCHITECTURE DESCRIPTION

The FPGA-based [5] microstep stepper motor control can be shown in block diagram as in Fig. 5.

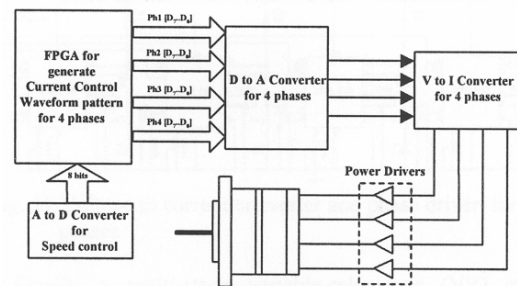


Fig. 5 Block diagram of FPGA-based stepper motor control

From Fig. 5 shows the components used for experiment that consists of major parts as follows, the analog to digital converter (ADC0804) is used for converting variable DC

voltage to 8 bits digital output for loadable clock frequency divider on FPGA to control the clock speed which result in motor speed.

FPGA is an important component used to control the phase currents to follow by microstep current references. The microstep current references can be found by (7) and (9) for linear approximations, and (12) and (14) for sinusoidal approximations, respectively. The obtained values are converted into suitable 8 bits binary numbers and stored in look-up tables (LUT's) for each phase. The up-down counter is used for each LUT's addressing, direction (clockwise or counter-clockwise) can be determined by count-up or count-down. In Fig. 6 shows the microstep controller which regular step angle was subdivided by 16.

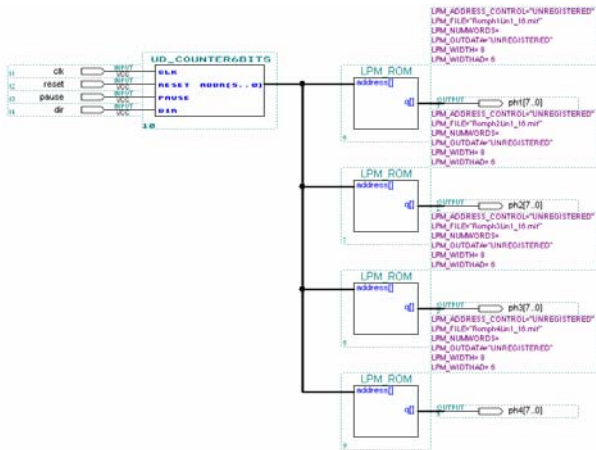


Fig.6 The FPGA-based microstep controller for $m=16$

In the case of $m=16$, each of LUT's have 64 addresses. Also, must be used 6 bits up-down counter for addressing. The counter can be modeled with VHDL and each of LUT's can be replaced with LPM_ROM (Library of Parameterized Modules) in MAX+PlusII program which the compiler automatically implements suitable portions of this function in EABs (Embedded Array Blocks) in FLEX10K devices. The current references of linear approximations and sinusoidal approximations for $m=16$ can be shown the waveform patterns as follow in Fig. 7 and 8, respectively.

Fig. 9 shows the simulation result of microstep controller for $m=16$. The *dir* input used for determining motor direction (cw or ccw), *reset* input used to reset the counter so that all addresses of each LUT's will be 0 and all values contained at address 0 of each phase will be output of FPGA, *pause* input used for holding the state of counter so that the output of each LUT's will be held until this input inactive.

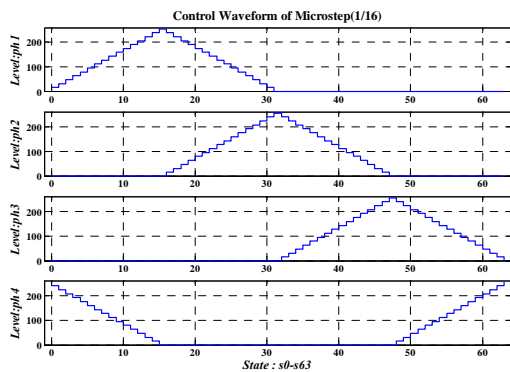


Fig. 7 Controlling waveform of linear approximations

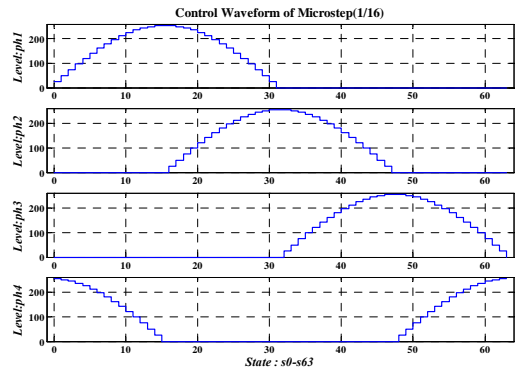


Fig.8 Controlling waveform of sinusoidal approximations



Fig. 9 Simulation result of microstep controller

The current pattern output of each LUT's from FPGA will be converted to analog signal by digital to analog converter (MC1408) as the circuits shown in Fig. 10.

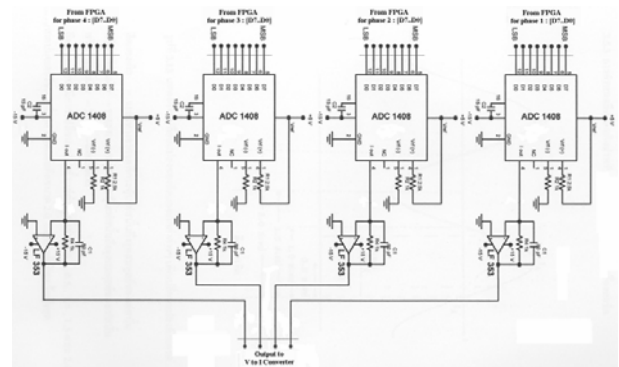


Fig. 10 Digital to analog converter for 4 phases

The output of digital to analog converter will be converted to current by voltage to current converter (XTR110) and uses MOSFET for phase drive circuits as shown in Fig. 11.

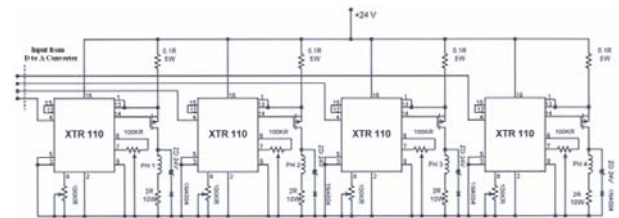


Fig. 11 Voltage to current converter and phase driver for 4 phases

Finally, a multi-stack variable-reluctance (VR) stepper motor of Sanyo Denki 103-770 series, Type 103-770-18, 1.8°/step was used in the experiments.

4. SYSTEM IMPLEMENTATION AND EXPERIMENTAL RESULTS

An EPF10K20RC240-4 device in FLEX10K device family used for circuit synthesis. The FPGA-based microstep controller used in experiment was subdivided the regular step by $m=2, 4, 8, 16$ and 32 microsteps, respectively. Table 1 shows the device and timing summary of microstep controller.

Table 1 Device and timing summary for various of m

	1/2	1/4	1/8	1/16	1/32
Logic cells	5	9	13	17	21
Memory bits	256	512	1024	2048	4096
Max. Frequency (MHz)	113.63	70.42	67.56	59.52	46.94

In Table 1 shows amount of logic cells used for implementation of 3, 4, 5, 6 and 7 bits up-down counter, respectively. Memory bits used for implementation of all LUT's for $m=2, 4, 8, 16$ and 32 , respectively and timing summary shows the maximum frequency of synthesized circuits.

Fig. 12 shows the microstep current reference waveform which can be found by (7) and (9) for linear approximation, this experimental result is correspondence to simulation result in Fig. 3. Fig. 13 shows the microstep current reference waveform which can be found by (12) and (14) for sinusoidal approximation, this experimental result is correspondence to simulation result in Fig. 4.

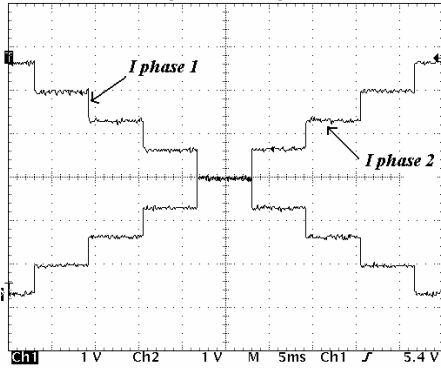


Fig. 12 Current waveform for $m=8$ (linear approximation)

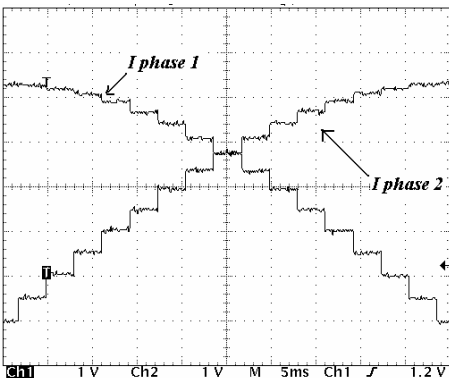


Fig. 13 Current waveform for $m=16$ (sinusoidal approximation)

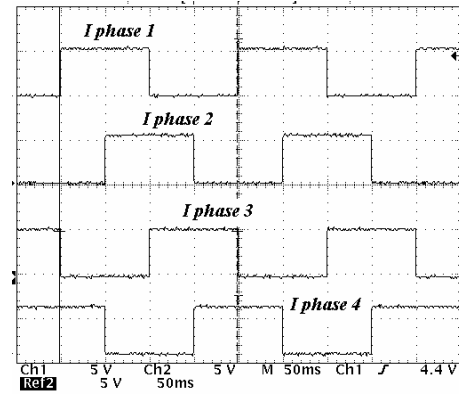


Fig. 14 Current control signal for full-step 2 phase mode

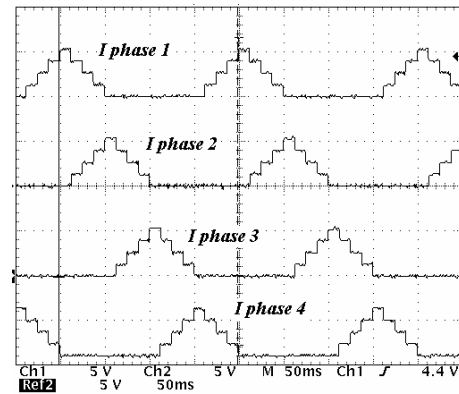


Fig. 15 Current control signal for $m=4$ (linear approximation)

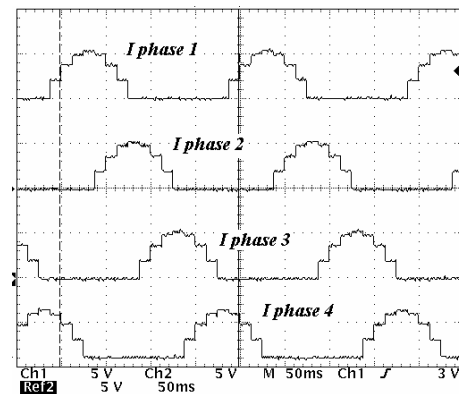


Fig. 16 Current control signal for $m=4$ (sinusoidal approximation)

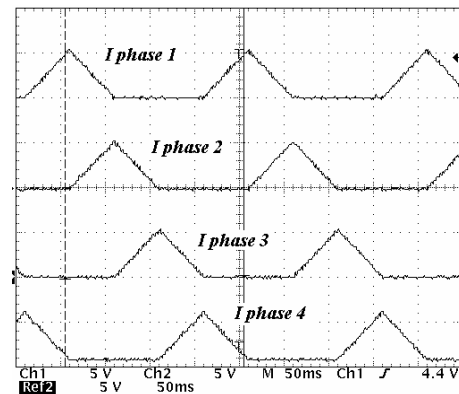


Fig. 17 Current control signal for $m=16$ (linear approximation)

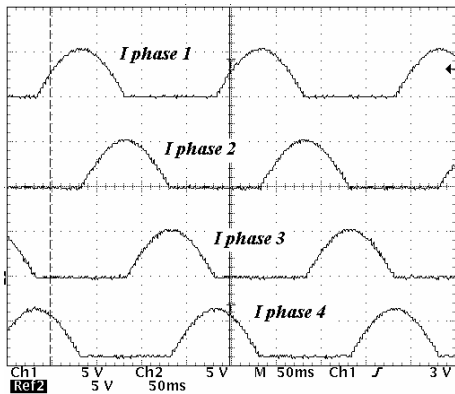


Fig. 18 Current control signal for $m=16$ (sinusoidal approximation)

Fig. 14 shows the control signal for regular step angle is $1.8^\circ/\text{step}$. Fig. 15 and 16 show the control signal that was subdivided the regular step angle by 4 for linear and sinusoidal approximation, respectively. Finally, Fig. 17 and 18 shows control signal that was subdivided the regular step angle by 16 for linear and sinusoidal approximation, respectively.

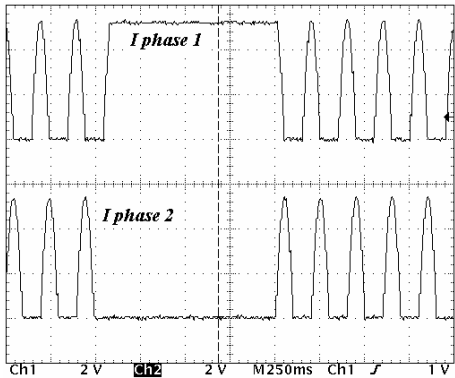


Fig. 19 Control signal when *reset* is active

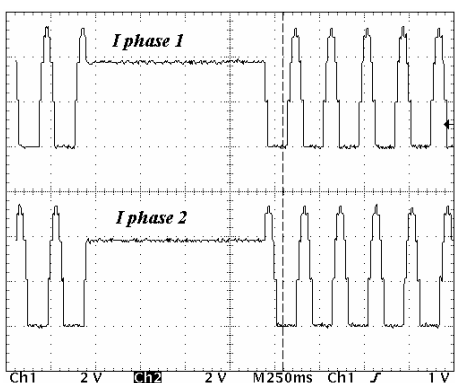


Fig. 20 Control signal when *pause* is active

Fig. 19 shows the control signal (only phase 1 and 2) when the reset signal is active, the contained value in address 0 of each LUT's will appear as output. Fig. 20 shows the control signal (only phase 1 and 2) when pause signal is active, this signal is used for holding the state of counter so that the output of each LUT's will be held.

5. CONCLUSIONS

This paper uses FPGA in the design and uses VHDL for describing the behavior of proposed microstep controller. The microstep current references waveform can be found by static torque-displacement approximation with linear and sinusoidal function. The experimental results are ensured to produce the current control signals. The difference between sinusoidal and linear approximation is the accuracy of obtained microstep angle which the sinusoidal approximation have the accuracy more than linear approximation [3-4]. Moreover, in practical the motor have the effects of magnetic saturation which result in nonlinearity in magnetic circuit and torque characteristics for each phase at displacement angle not identical. Also, all microsteps will be not equal in angle. Therefore, the best way to obtained much more accuracy in microstep angle is microstep current reference signals must be found by direct tested from practical motor characteristics [4], and since the nature of stepper motor control is open-loop, also can use closed-loop current control to current feedback when compared with the microstep reference current signal for controlling the phase currents too.

REFERENCES

- [1] P. P. Acarnley, Stepping Motors: A Guide to Modern Theory and Practice, IEE Control Engineering Series 19, Peter Peregrinus Ltd., 1982.
- [2] T. Kenjo, Stepping Motors and Their Microprocessor Controls, Monographs in Electrical and Electronic Engineering, Oxford Univ. Press, 1986.
- [3] M. F. Rahman, A. N. Poo and C. S. Chang, "Approaches to Design of Ministepping Step Motor Controllers and Their Accuracy Considerations," IEEE Trans. Industrial Electronics, vol. IE-32, No. 3, pp. 229-233, August 1985.
- [4] M. F. Rahman and A. N. Poo, "An Application Oriented Test Procedure for Designing Microstepping Step Motor Controllers," IEEE Trans. Industrial Electronics, vol. 35, No. 4, pp. 542-546, November 1988.
- [5] D. Carrica, M. A. Funes and S. A. Gonzalea, "Novel Stepper Motor Controller Based on FPGA Hardware Implementation," IEEE/ASME Trans. Mechatronics, vol. 8, No. 1, pp.120-124, March 2003.